ESC European Society of Cardiology

Cardiovascular Research (2024) **120**, 735–744
https://doi.org/10.1093/cvr/cvae042

The electrophysiologic effects of *KCNQ1* extend beyond expression of I_{Ks}: evidence from genetic and pharmacologic block

Yuko Wada [1], Lili Wang[1], Lynn D. Hall[1], Tao Yang[1], Laura L. Short[1], Joseph F. Solus[1], Andrew M. Glazer[1], and Dan M. Roden [1,2]*

[1]Department of Medicine, Vanderbilt University Medical Center, 2215B Garland Ave, 1285 MRBIV, Nashville, TN 37232, USA; and [2]Departments of Medicine, Pharmacology, and Biomedical Informatics, Vanderbilt University Medical Center, 2215B Garland Ave, 1285 MRBIV, Nashville, TN 37232, USA

Received 6 April 2023; revised 22 January 2024; accepted 1 February 2024; online publish-ahead-of-print 5 March 2024

Time of primary review: 31 days

See the editorial comment for this article 'Interactions between KCNQ1 and KCNH2 may modulate the long QT type 1 phenotype', by K.E. Odening, https://doi.org/10.1093/cvr/cvae074.

Aims

While variants in *KCNQ1* are the commonest cause of the congenital long QT syndrome, we and others find only a small I_{Ks} in cardiomyocytes from human-induced pluripotent stem cells (iPSC-CMs) or human ventricular myocytes.

Methods and results

We studied population control iPSC-CMs and iPSC-CMs from a patient with Jervell and Lange-Nielsen (JLN) syndrome due to compound heterozygous loss-of-function (LOF) *KCNQ1* variants. We compared the effects of pharmacologic I_{Ks} block to those of genetic *KCNQ1* ablation, using JLN cells, cells homozygous for the *KCNQ1* LOF allele G643S, or siRNAs reducing *KCNQ1* expression. We also studied the effects of two blockers of I_{Kr}, the other major cardiac repolarizing current, in the setting of pharmacologic or genetic ablation of *KCNQ1*: moxifloxacin, associated with a very low risk of drug-induced long QT, and dofetilide, a high-risk drug. In control cells, a small I_{Ks} was readily recorded but the pharmacologic I_{Ks} block produced no change in action potential duration at 90% repolarization (APD_{90}). In contrast, in cells with genetic ablation of *KCNQ1* (JLN), baseline APD_{90} was markedly prolonged compared with control cells (469 ± 20 vs. 310 ± 16 ms). JLN cells displayed increased sensitivity to acute I_{Kr} block: the concentration (μM) of moxifloxacin required to prolong APD_{90} 100 msec was 237.4 [median, interquartile range (IQR) 100.6–391.6, $n = 7$] in population cells vs. 23.7 (17.3–28.7, $n = 11$) in JLN cells. In control cells, chronic moxifloxacin exposure (300 μM) mildly prolonged APD_{90} (10%) and increased I_{Ks}, while chronic exposure to dofetilide (5 nM) produced greater prolongation (67%) and no increase in I_{Ks}. However, in the siRNA-treated cells, moxifloxacin did not increase I_{Ks} and markedly prolonged APD_{90}.

Conclusion

Our data strongly suggest that *KCNQ1* expression modulates baseline cardiac repolarization, and the response to I_{Kr} block, through mechanisms beyond simply generating I_{Ks}.

* Corresponding author. Tel: +1 615 322 0067; fax: +1 615 343 4522, E-mail: dan.roden@vumc.org

Graphical Abstract

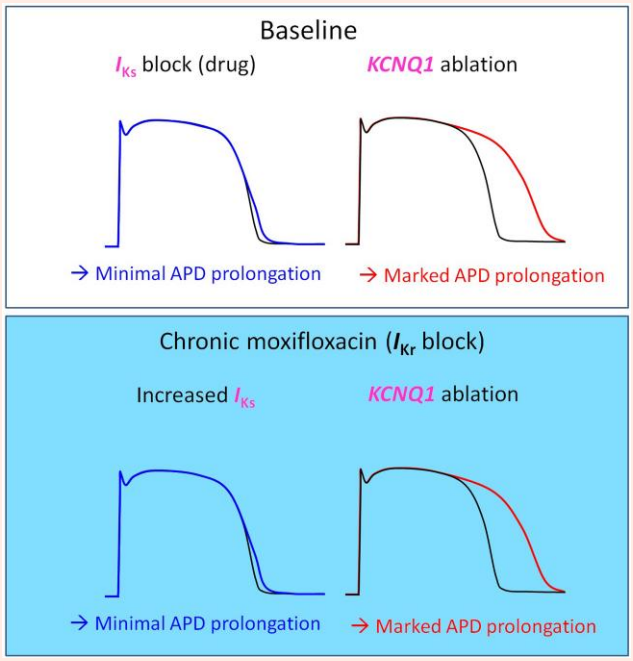

Keywords Repolarization reserve • *KCNQ1* • I_{Ks} • I_{Kr} • Long QT

1. Introduction

Cardiac repolarizing ion currents tightly govern normal ventricular repolarization, clinically captured as the QT interval on the ECG, in the human heart. The slowly and rapidly activating delayed rectifier potassium currents, I_{Ks} and I_{Kr}, respectively, play a major role in repolarization in humans, and these are nearly absent in small mammals such as mouse or rat.[1,2] Loss-of-function (LOF) variants in *KCNQ1* and *KCNH2*, encoding K_V7.1 and hERG/K_V11.1 to generate I_{Ks} and I_{Kr}, respectively, cause Type 1 and Type 2 congenital long QT syndrome (cLQTS), together accounting for >90% of cLQTS cases.[3,4] In the more severe Jervell and Lange-Nielsen (JLN) syndrome, patients are usually homozygotes or compound heterozygotes for *KCNQ1* LOF variants.[5,6]

Pharmacologic block of I_{Kr} prolongs QT intervals and when exaggerated can result in the drug-induced long QT syndrome (diLQT), which includes marked QT prolongation and the morphologically distinctive ventricular tachycardia torsades de pointes (TdP).[7] I_{Kr}/hERG block prolongs action potential duration (APD), an *in vitro* correlate of the QT interval, in multiple cardiac cell types including rabbit myocytes[8,9] and human cardiomyocytes developed from induced pluripotent stem cells (iPSC-CMs).[10–13]

LOF variants in *KCNQ1* are the most common finding in cLQTS[14,15] and genetic manoeuvres reproduce the cLQTS phenotype in multiple animal and human experimental models.[16–20] Pharmacologic block of I_{Ks} is, however, reported to have little or no effect on APDs in cardiomyocytes from various species (isolated rabbit Purkinje fibres, dog ventricular myocytes, isolated human ventricular myocytes, and human iPSC-CMs).[8,21–25] Thus, the mechanism whereby LOF variants of *KCNQ1* cause cLQTS but I_{Ks} block seems to have little effect on APD remains ill-defined. Scattered reports have suggested that K_V7.1, in addition to acting as the pore-forming subunit for I_{Ks}, can also act as a chaperone to traffic hERG to the cell surface.[26–28]

Here we show that the pharmacologic block of I_{Ks} produces little change in APD in control iPSC-CMs, while multiple approaches that genetically ablate *KCNQ1* produce marked APD prolongation. Further, we find that moxifloxacin, a drug which rarely triggers diLQT, not only blocks I_{Kr} as expected but also increases I_{Ks} and this effect limits APD prolongation. In contrast, dofetilide, which carries a higher risk for diLQT, does not increase I_{Ks} and prolongs APD to a greater extent. These data provide support for an emerging general concept that cardiomyocytes can generate compensatory changes to limit the extent to which drug challenges or genetic lesions prolong cardiac repolarization and generate long QT-related arrhythmias.

2. Methods

Detailed study methods are presented in Supplementary material online, Methods. Upon generation of iPSCs, a healthy volunteer and a patient gave written informed consent prior to inclusion in the study under institutional review board (IRB) approval in accordance with the Declaration of Helsinki. All drugs tested in this study are commercially available and listed in Supplementary material online, *Table S1*. The study was approved by the IRB and the subjects whose iPSCs were generated for the study gave written informed consent. Key recordings were obtained from three or more independent differentiation batches to minimize batch-to-batch variability and presented as *n*/*N*, where *n* and *N* indicate the number of recordings and the number of independent differentiation batches, respectively.

All data are expressed as mean ± SE unless otherwise indicated. $[Mox]_{\Delta 100ms}$ values were non-normally distributed by the Shapiro–Wilk *W* test but log-normally distributed by the Kolmogorov *D* test and so were log-transformed for analysis. For normally distributed continuous variables, two-tailed *t*-tests (paired or unpaired, as appropriate) or ANOVA were employed with Tukey's test if an ANOVA found differences among groups. For non-normally distributed continuous variables, the Mann–Whitney *U* test or Kruskal–Wallis test was employed. $P < 0.05$ was considered as significant. Prism 5.0 (GraphPad Software) and JMP9.0 were used for analysis and illustration generation.

3. Results

3.1 Pharmacologic block of I_{Ks} had no effect on baseline repolarization in contrast to genetic ablation

To pharmacologically block I_{Ks}, we used the specific blocker HMR-1556, which has been used to study I_{Ks} in rabbit hearts,[30] dog ventricular myocytes,[31] and human cardiomyocytes,[22] at a high concentration (0.5 μM): the IC_{50} for I_{Ks} block is reported to be 0.01 μM[31] and submicromolar HMR-1556 does not block transient outward current (I_{to}), I_{Kr}, and L-type calcium current in dog ventricular myocytes.[31] Throughout this text and figures, we report APD data (as APD at 90% repolarization, APD_{90}) at a pacing rate of 0.5 Hz and provide other parameters in the data supplement. HMR-1556 did not prolong APD_{90} with acute exposure [from 282 ± 28 to 276 ± 27 ms ($n/N = 11/5$), $P = 0.55$] (*Figure 1A*) or with chronic exposure for 24–48 h [315 ± 22 ms ($n/N = 36/5$) vs. control cells 310 ± 16 ms ($n/N = 56/11$), $P = 0.72$] (*Figure 1B*, Supplementary material online, *Table S2*). With protein kinase A (PKA) stimulation by 3-isobutyl-1-methylxanthine (IBMX) 200 μM and forskolin 10 μM, acute exposure to HMR-1556 produced marginal APD_{90} prolongation, 7% (16.2 ± 6.1 msec) at 2 Hz (*Figure 1C* and *D*). This is in keeping with previous reports that human ventricular myocytes display small I_{Ks} even with PKA stimulation.[22,32,33]

We next measured baseline repolarization in iPSC-CMs generated from a patient with JLN who carried compound heterozygous variants of *KCNQ1*; a paternally inherited R518X in exon 12 and a *de novo* 52 bp insertion in exon 15, as previously described.[34] Expression of major cardiac ion channels was no different between the control and JLN cells, except for *KCNQ1* and *KCNH2* (see Supplementary material online, *Figure S1*). Reverse transcriptase-polymerase chain reaction and RNA-seq in the JLN iPSC-CMs demonstrated nonsense-mediated messenger RNA decay caused by the R518X and exon 15 skipping caused by the *de novo* indel (see Supplementary material online, *Figure S2*). JLN cells showed markedly prolonged APD_{90} compared to control cells at baseline [469 ± 20 ($n/N = 59/10$), $P < 0.0001$ vs. control cells] (*Figure 1B*).

I_{Ks} was measured as the current sensitive to HMR-1556 (0.5 μM) and was clearly detectable in control cells at baseline [0.70 ± 0.12 pA/pF at +40 mV ($n/N = 27/6$)] (*Figure 1E*). With acute exposure to PKA activators (IBMX and forskolin), I_{Ks} was increased three-fold to 1.6 ± 0.26 pA/pF at +40 mV ($n/N = 10/3$, $P = 0.001$ vs. untreated control cells). On the other hand, in JLN cells, I_{Ks} was not detectable at baseline [0.09 ± 0.02 pA/pF at +40 mV ($n/N = 10/5$), data not shown in the figure] nor with the PKA activators [0.01 ± 0.04 pA/pF at +40 mV ($n/N = 8/3$)] (*Figure 1F–H*). Unlike PKA activators, a putative I_{Ks} activator, isoproterenol, did not acutely increase I_{Ks} at conventional concentration (1 μM) nor high concentration (10 μM) in control iPSC-CMs, while the effect of isoproterenol (10 μM) on action potential shortening was clear (see Supplementary material online, *Figure S3*).

Taken together, although I_{Ks} is recorded small in iPSC-CMs, loss of I_{Ks} resulting from genetic loss of *KCNQ1* (in the JLN cells) caused markedly impaired repolarization, whereas pharmacologic full-block of I_{Ks} had minimal effects even with PKA stimulation.

3.2 Genetic loss of I_{Ks} reduced repolarization reserve shown by acute I_{Kr} block

We next tested the sensitivity of JLN cells to acute I_{Kr} block. We and others have previously shown that chronic exposure to some I_{Kr} blockers, such as dofetilide (which is known to confer a high risk for diLQT) increases late sodium current ($I_{Na\text{-}L}$).[35,36] Accordingly, in these experiments, we used moxifloxacin, an antibiotic associated with a low risk for diLQT but known to block I_{Kr} and exert minimal effects on other ion currents.[35,37,38] The IC_{50} for moxifloxacin block of I_{Kr} in control cells was 221 ± 146 μM (see Supplementary material online, *Figure S4A–C*). To quantitate sensitivity to I_{Kr} block, we exposed cells to increasing moxifloxacin concentrations (2–3 min/concentration) to establish the concentration that prolonged APD_{90} by 100 ms [$(Mox)_{\Delta 100ms}$] using log-linear interpolation (*Figure 2A–D*). The baseline *KCNH2* expression level in the JLN cells was lower than that in the control cells, while I_{Kr} amplitude was increased in the JLN cells (see Supplementary material online, *Figures S1 and S5*).

JLN cells displayed much greater sensitivity to I_{Kr} block than the control cells: median $[Mox]_{\Delta 100ms}$ in control cells and JLN cells was 237.4 μM [interquartile range (IQR): 100.6–391.6] ($n = 7/3$) and 23.7 μM [IQR: 17.3–28.7] ($n/N = 11/5$), respectively ($P = 0.0008$) (*Figure 2E*). Chronic pharmacologic block of I_{Ks} by HMR-1556 (0.5 μM for 24–48 h) did not change $[Mox]_{\Delta 100ms}$ in the control cells [107.6 μM (IQR: 40.8–283.3), $n/N = 8/3$, $P = 0.40$ vs. control cells; $P = 0.0008$ vs. JLN cells] (*Figure 2E*). Because a high concentration of moxifloxacin was required to prolong APD_{90} in the control cells, we also compared absolute changes of APD_{90} (ΔAPD_{90}) at a fixed low dose moxifloxacin (30 μM) in the control cells, JLN cells, and the control cells pre-treated with HMR-1556, and these were 17.9 ± 7.6 ms ($n/N = 9/3$), 95.5 ± 15.9 ($n/N = 13/6$), and 18.3 ± 6.3 ms ($n/N = 8/3$), respectively ($P = 0.0003$ between control and JLN cells; $P = 0.0008$ between JLN and HMR-1556-treated control cells; $P = 0.74$ between control and HMR-1556-treated control cells) (*Figure 2F*). These data show that with genetic loss of *KCNQ1*, the cells' ability to maintain repolarization in the face of acute I_{Kr} block was severely impaired, but this was not seen with pharmacologic block of I_{Ks}.

3.3 Chronic I_{Kr} block by moxifloxacin minimally prolonged APD in iPSC-CMs but dofetilide did not

Although acute exposure to moxifloxacin significantly prolonged APD_{90} (*Figure 2G*), this effect was blunted with chronic exposure (300 μM, 24–48 h) in the control cells: APD_{90} was prolonged only 10% [to 342 ± 23 ms ($n = 27/4$), $P = 0.18$ vs. untreated control cells, *Figure 3A*, Supplementary material online, *Table S3*]. In these cells, I_{Ks} was strikingly increased after chronic exposure to moxifloxacin in a concentration-dependent manner [0.4 ± 0.05 pA/pF without moxifloxacin ($n = 4$), 0.7 ± 0.2 pA/pF with 30 μM ($n = 4$), 1.3 ± 0.3 pA/pF with 300 μM ($n = 5$)] in cells from the same differentiation batch, *Figure 3B* and *C*). The effect of chronic moxifloxacin exposure on I_{Ks} was evident after 24 h of treatment and lasted for at least 48 h (see Supplementary material online, *Figure S6*). We analysed data obtained between 24 and 48 h. Unlike moxifloxacin, chronic dofetilide exposure did not increase I_{Ks} at neither 5 nM nor 20 nM, near IC_{50} for I_{Kr} (see Supplementary material online, *Figure S7*).

To determine whether this increase in I_{Ks} was also seen with dofetilide, we first established the IC_{50} for acute I_{Kr} block as 19.9 nM (see Supplementary material online, *Figure S4D*). Unlike moxifloxacin, chronic exposure to dofetilide (5 nM, a concentration that produced minimal increases in $I_{Na\text{-}L}$ in our previous work[35]) significantly prolonged APD_{90} in the control cells [518 ± 53 ms ($n/N = 20/4$), $P = 0.0002$ vs. untreated cells; $P = 0.01$ vs. MOX-treated cells, *Figure 3A* and Supplementary material online, *Table S3*]. Further, also unlike moxifloxacin, chronic exposure to dofetilide did not increase I_{Ks} [0.5 ± 0.1 pA/pF ($n/N = 16/4$), $P = 0.13$ vs. untreated cells] (*Figure 3D*). Chronic exposure of JLN cells to moxifloxacin markedly prolonged APD_{90} [657 ± 74 ms ($n/N = 23/3$), $P = 0.018$ vs. untreated JLN cells, *Figure 3E* and Supplementary material online, *Table S4*]. Quantitative polymerase chain reaction (qPCR) showed that chronic moxifloxacin significantly increased both *KCNQ1* ($P = 0.0006$) and *KCNH2* transcripts ($P = 0.0006$) while there was minimal effect with dofetilide (*KCNQ1*, $P = 0.05$; *KCNH2*, $P = 0.56$) ($n = 5$–7) (*Figure 3F*). We did not observe significant changes in the gene expression level of other major ion channels and subunits (*SCN5A*, *KCNE1*, *KCNJ2*, *CACNA1C*) (see Supplementary material online, *Figure S8*).

As we observed an increase in *KCNH2* transcripts with the I_{Kr} blockers, we attempted to quantify the residual I_{Kr} after chronic exposure to the I_{Kr} blockers. Residual I_{Kr} was assessed as an E-4031-sensitive current after the

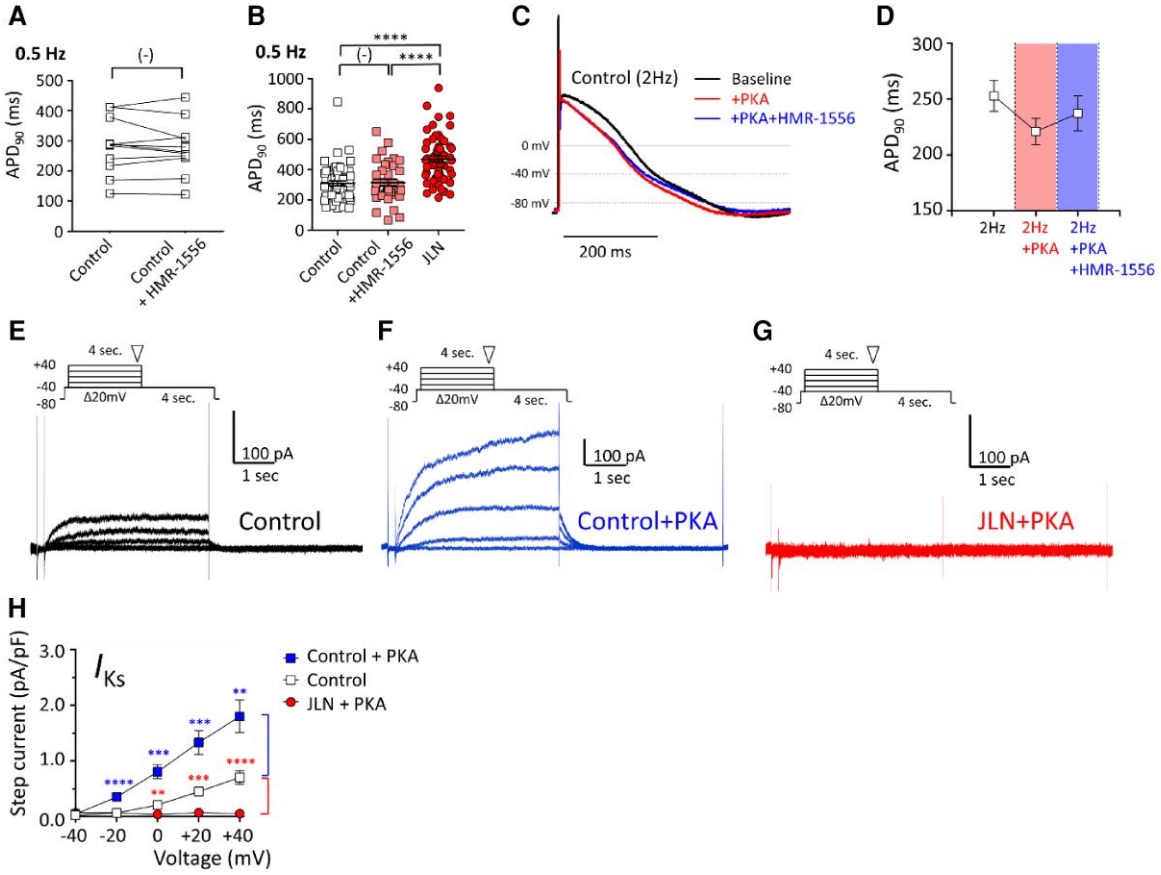

Figure 1 Effect of pharmacological block and genetic loss of *KCNQ1* on action potential durations and I_{Ks}. (*A*) Acute pharmacological block of I_{Ks} in control cells. A high concentration of the I_{Ks}-specific blocker HMR-1556 produced no change in APD_{90} at 0.5 Hz pacing (paired recordings, $P = 0.55$ by paired *t*-test). (*B*) Baseline APD_{90} at 0.5 Hz in untreated control cells (open squares, $n/N = 56/11$), control cells pre-treated with HMR-1556 for 24–48 h (pink squares, $n/N = 36/5$), and in untreated JLN cells (red circles, $n/N = 59/10$). (*C*) Representative traces of action potentials in the same control cell (at 2 Hz) during acute exposure to PKA activators (IBMX and forskolin, red trace) followed by I_{Ks} block with HMR-1556 (blue trace). (*D*) Summary APD_{90} data during acute exposure to PKA activators followed by HMR-1556 ($n/N = 14/2$). (*E–G*) Representative traces of I_{Ks} in a control cell without PKA activation (*E*), control cell with PKA activation (*F*), and a JLN cell with PKA activation (*G*) by IBMX and forskolin. Insets show the stimulus protocol. An inverted triangle in the inset indicates where the step current of I_{Ks} was measured. (*H*) The current–voltage relationship for activation of I_{Ks} measured at the end of the step in JLN cells with PKA activators (red circles, $n/N = 8/3$), control cells without PKA activators (open squares, $n/N = 27/6$), and control cells with PKA activators (blue squares, $n/N = 10/3$). The numbers of data points are expressed as *n/N*, where *n* indicates number of recordings and *N* indicates number of differentiation batches. (–) not significant, $^{**}P < 0.01$, $^{***}P < 0.001$, $^{****}P < 0.0001$ by Kruskal–Wallis test unless otherwise specified. APD_{90}, action potential duration at 90% repolarization; JLN, Jervell and Lange-Nielsen; IBMX, 3-isobutyl-1-methylxanthine; PKA, protein kinase A.

drug was washed out with Tyrode's solution before recording (there was no I_{Kr} recorded when the drug was not washed out). We observed slightly reduced I_{Kr} in the cells pre-treated with moxifloxacin after 11–20 min of wash-out (at −10 mV, $n = 7$, $P = 0.049$ vs. untreated cells) (see Supplementary material online, *Figure S9*). I_{Kr} in the cells pre-treated with dofetilide was not different from untreated cells after 13–38 min of washout.

A western blot in control iPSC-CMs showed a trend of increased $K_V7.1$ with both moxifloxacin and dofetilide [3.0 ± 1.38-fold ($P = 0.06$) and 3.0 ± 1.63-fold ($P = 0.06$) vs. untreated cells, respectively]. However, neither I_{Kr} blocker increases hERG (1.36 ± 0.37-fold increase by moxifloxacin; 3.5 ± 1.48-fold increase by dofetilide) (see Supplementary material online, *Figure S10*).

Taken together, these data indicate that the limited prolongation of repolarization with chronic moxifloxacin challenge reflects at least in part increased I_{Ks}, through a transcriptional mechanism, an effect not seen with dofetilide or in JLN, which both carry a higher risk of diLQT.

3.4 Suppression of *KCNQ1* expression phenocopied JLN sensitivity to I_{Kr} block

Pharmacologic ablation of I_{Ks} did not affect baseline repolarization, whereas the JLN cells show that genetic ablation prolonged APD_{90} and made the cells more sensitive to the APD prolonging effects of I_{Kr} block. To further test the effects of genetic ablation, we determined the APD_{90} prolonging effect of moxifloxacin in control cells pre-treated with non-targeting small interfering RNA (Negative siRNA) or siRNAs targeting exon1 and 6 of *KCNQ1* (KCNQ1-KD). KCNQ1-KD reduced *KCNQ1* transcripts by 86% assessed by qPCR ($N = 4$, $P = 0.002$) (*Figure 4A*) and reduced I_{Ks} by 68% compared to the cells pre-treated with Negative siRNA [0.22 ± 0.05 vs. 0.68 ± 0.12 pA/pF at 40 mV ($n/N = 7$–11/3), $P = 0.001$] (*Figure 4B* and *C*). In cells treated with siRNAs (KCNQ1-KD), baseline APD_{90} was prolonged to an extent similar to that seen in JLN cells [541 ± 55 ms ($n/N = 19/4$), $P < 0.0001$ vs. control cells; $P = 0.31$ vs. JLN cells, *Figure 4D*]. Unlike control cells, chronic exposure to moxifloxacin (300 μM) did not increase I_{Ks}

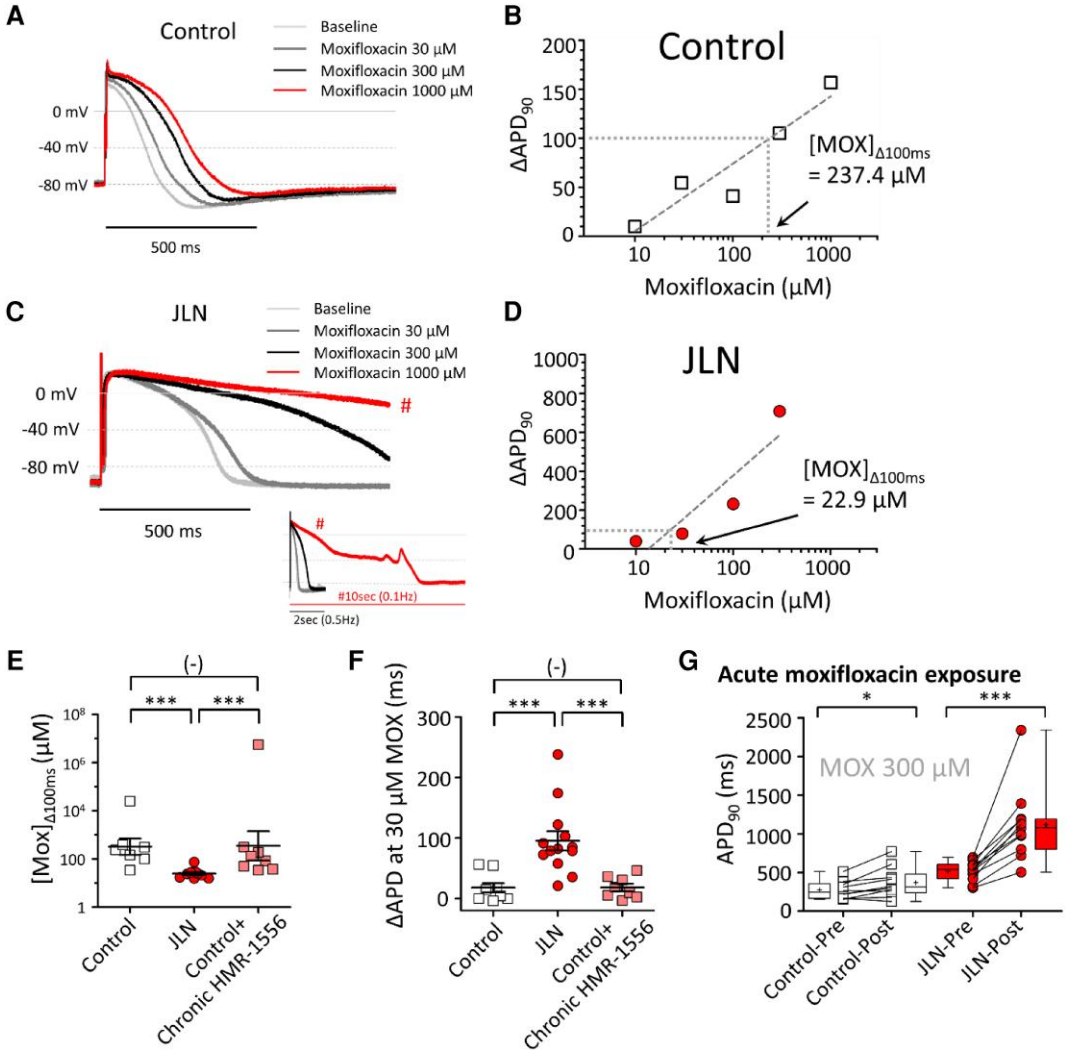

Figure 2 Effect of acute exposure to moxifloxacin in control and JLN iPSC-CMs. (*A*) Representative action potential traces during acute exposure to increasing concentrations of moxifloxacin (2–3 min/concentration) in a control cell (at 0.5 Hz). (*B*) Log-linear interpolation to determine moxifloxacin concentration that prolonged APD_{90} by 100 ms [$(MOX)_{\Delta 100ms}$] in the control cell shown in (*A*). (*C*) Representative action potential traces during moxifloxacin exposure in a JLN cell. The trace at 1000 μM moxifloxacin (red) was longer than 2000 msec at 0.5 Hz pacing (#) and showed triggered activity/early afterdepolarizations, as shown in an inset in a full trace obtained at 0.1 Hz pacing. (*D*) Log-linear interpolation of the JLN cell data shown in (*C*). Note the difference in scale on the *Y*-axis between panels B (maximum 200 ms) and D (maximum 1000 ms). (*E*) $[MOX]_{\Delta 100ms}$ (note log-scale) in control (open squares, $n/N = 7/3$), JLN (red circles, $n/N = 11/4$), and control cells pre-treated with HMR-1556 (pink squares, $n/N = 8/3$). (*F*) Absolute change in APD_{90} (ΔAPD_{90}) with acute exposure to 30 μM moxifloxacin in control (open squares, $n/N = 8/4$), JLN (red circles, $n/N = 13/5$), and control cells pre-treated with HMR-1556 (pink squares, $n/N = 8/3$). (*G*) Acute effect of high concentration moxifloxacin at 300 μM on APD_{90} (at 0.5 Hz). $n/N = 10–11/4–5$. Comparison was made using a paired *t*-test. (–) not significant, ***$P < 0.001$ by Kruskal–Wallis test otherwise specified.

($n/N = 7/3$, $P = 0.47$ vs. untreated KCNQ1-KD) (*Figure 4C*) and markedly prolonged APD_{90} [1057 ± 89 ms ($n/N = 16/2$), $P < 0.0001$ vs. control cells pre-treated with moxifloxacin; $P = 0.0007$ vs. JLN cells pre-treated with moxifloxacin] (*Figure 4E*). These results support the idea that genetic ablation of *KCNQ1* expression markedly enhances sensitivity to the action potential prolonging effects of I_{Kr} block by moxifloxacin.

3.5 Effect of a common LOF genetic variant on I_{Ks} and APD_{90} response to I_{Kr} blocker challenge

Next, we tested whether a common variant of *KCNQ1* that has been associated with diLQT generates the diLQT phenotype through the loss of the dynamic increase in I_{Ks} that we see with I_{Kr} block by moxifloxacin.

KCNQ1 G643S (rs1800172) is the second most common missense variant in *KCNQ1* in the population database gnomAD (minor allele frequency: 4.6% in East Asians; 2.1% in Africans; 0.02% in Europeans). Reports from Asian cohorts have associated this variant with diTdP and drug-related sudden death despite nearly normal baseline I_{Ks} when the variant is studied in heterologous overexpression in both homozygous and heterozygous states.[39,40] We, therefore, generated and studied homozygous G643S cells (isogenic to the population control cells, Supplementary material online, *Figure S11*) to determine the extent to which the increase in I_{Ks} and limited APD prolongation generated by moxifloxacin challenge in control cells was also seen in G643S cells.

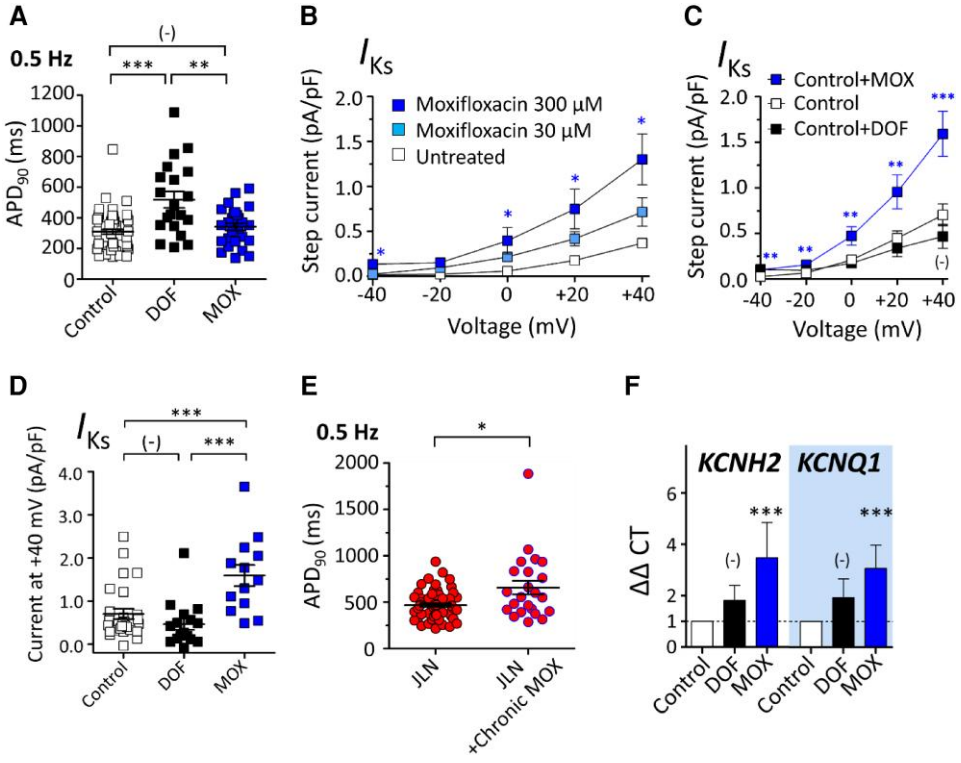

Figure 3 The effects of moxifloxacin and dofetilide on action potential duration, I_{Ks}, and *KCNH2* and *KCNQ1* transcripts in control and JLN iPSC-CMs. (*A*) The effect of chronic (24–48 h) exposure to moxifloxacin and dofetilide on APD_{90} in control cells (at 0.5 Hz). DOF: dofetilide at 5 nM (black squares, $n/N = 20/4$); MOX: moxifloxacin at 300 μM (blue squares, $n/N = 27/4$). The dotted line and gray band indicate the mean ± SE for control cells from *Figure 1B*. (*B*) I_{Ks} *I–V* relationship showed a dose-dependent effect of moxifloxacin in control cells isolated from identical differentiation batches: Untreated cells (open squares, $n = 4$); pre-treated with 30 μM moxifloxacin (light blue squares, $n = 4$); pre-treated with 300 μM moxifloxacin (blue squares, $n = 5$). (*C*) I_{Ks} *I–V* relationship in control cells pre-treated with moxifloxacin 300 μM (MOX, blue squares, $n/N = 13/5$) or dofetilide 5 nM (DOF, black squares, $n/N = 16/4$). Comparisons were made with control cells without treatment (control, open squares, $n/N = 27/6$). (*D*) I_{Ks} amplitude measured at +40 mV in untreated control cells (open squares, $n/N = 27/6$), pre-treated with DOF (black squares, $n/N = 16/4$), and with MOX (blue squares, $n/N = 13/5$). (*E*) The effect of chronic exposure to moxifloxacin 300 μM on APD_{90} in JLN cells (at 0.5 Hz) (red-filled blue circles, $n/N = 23/3$). The statistical comparison shown used Mann–Whitney *U* test between JLN cells and those pre-treated with moxifloxacin. (*F*) *KCNH2* and *KCNQ1* transcript levels during pre-treatment with I_{Kr} blockers ($n = 5–7$). (−) not significant, *$P < 0.05$, **$P < 0.01$, ***$P < 0.001$ by Kruskal–Wallis test otherwise specified.

Baseline APD_{90} was comparable in G643S cells with the control cells [322 ± 24 ms ($n/N = 17/3$), $P = 0.59$] (*Figure 5A*). However, unlike in control cells, chronic exposure to moxifloxacin (300 μM) significantly prolonged APD_{90} [641 ± 52 ms ($n = 18/3$), $P < 0.0001$ vs. control cells pre-treated with moxifloxacin] (*Figure 5A* and Supplementary material online, *Table S5*). Baseline I_{Ks} was similar in the control and G643S cells [0.42 ± 0.08 ($n/N = 15/3$) at +40 mV, $P = 0.08$ vs. control cells], and PKA activation significantly increased I_{Ks} to a similar extent (71 and 75% increase at +40 mV in control and G643S cells, respectively) (*Figure 5B* and *C*). However, the effect of chronic moxifloxacin treatment to increase I_{Ks} in control cells was absent in the G643S cells (*Figure 5D*). Unlike in the isogenic control cells, moxifloxacin did not increase *KCNQ1* transcripts in the G643S variant cells (see Supplementary material online, *Figure S12*).

4. Discussion

4.1 A refined understanding of long QT syndrome genetics: beyond single variants

Initial studies of the molecular genetics of cLQTS reinforced the first principle that QT prolongation is caused by reduced net outward repolarizing current, reflecting reduced repolarizing potassium current through $K_V7.1$ or hERG, increased late sodium current ($I_{Na\text{-}L}$), or occasionally increased calcium current.[7,41–46] Similarly, early studies defined I_{Kr} block as the predominant mechanism in diLQT. However, cLQTS variants are incompletely penetrant, not all I_{Kr} blockers carry the same liability for diLQT, and even high-risk I_{Kr} blockers such as dofetilide cause diLQT in only a small fraction of exposed patients. Thus, other factors must modulate the risk for QT prolongation and TdP in these settings. Those factors can be environmental (e.g. bradyarrhythmia or hypokalaemia), and an increasing set of data implicate single[47–50] or multiple[51] genetic variants as modulators of that variable risk. We have recently reported that iPSC-CMs carrying common *SCN5A* variants that increase $I_{Na\text{-}L}$ did not display the expected increase in APD_{90}, and the implicated underlying mechanism was a compensatory increase in I_{Kr}.[29] Notably, it was the availability of iPSCs, and the ability to perform DNA editing in those cells, that enabled that discovery.

4.2 What the present study demonstrates

As discussed above, multiple laboratories have reported only a small I_{Ks} in mammalian (including human) cardiomyocytes, and this is difficult to reconcile with the fact that *KCNQ1* LOF mutations are the commonest cause of cLQTS. Here, we used the power of iPSC-CMs to address this apparent paradox. We find that while a small I_{Ks} is readily recorded in population iPSC-CMs, its inhibition by the I_{Ks}-specific blocker HMR-1556 produced

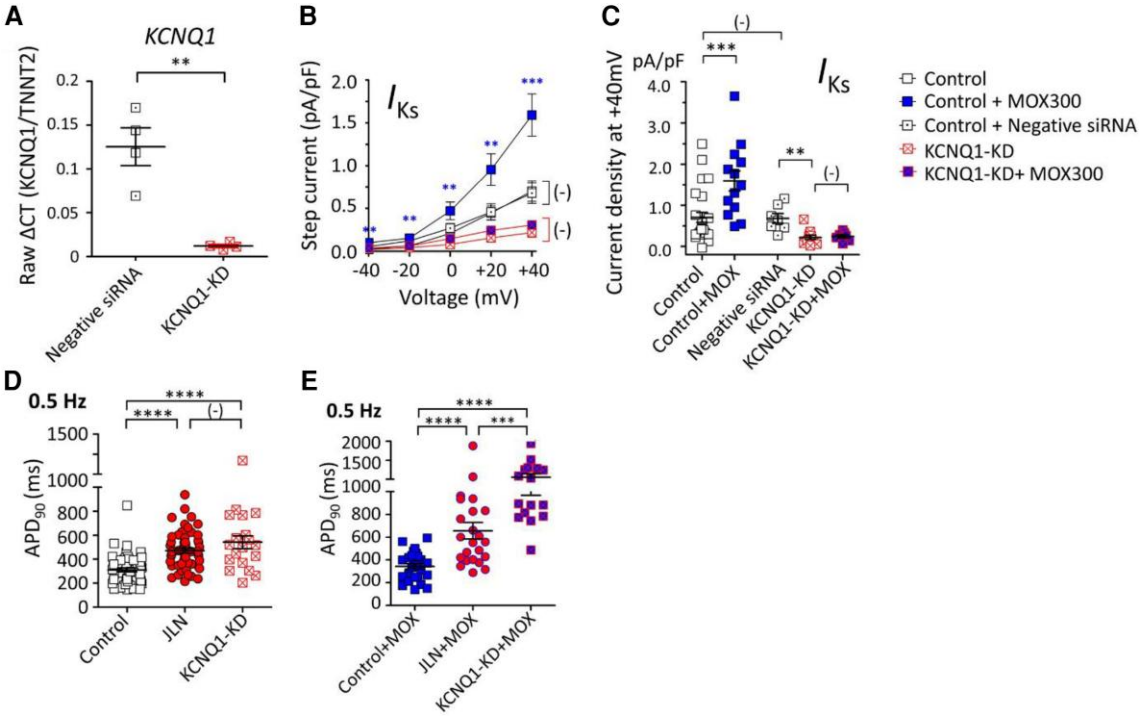

Figure 4 The effect of *KCNQ1* knock-down on I_{Ks} and action potential duration. (*A*) The efficiency of gene-specific knock-down of *KCNQ1* assessed by qPCR. Raw ΔCT values are plotted as relative expression normalized to *TNNT2* expression. Mann–Whitney *U* test was employed. (*B*, *C*) *I–V* relationship (*B*) and I_{Ks} densities at +40 mV (*C*) in control cells: untreated, pre-treated with moxifloxacin 300 μM, pre-treated with non-targeting siRNA (Negative siRNA), siRNA targeting both exon1 and exon6 of *KCNQ1* (KCNQ1-KD), and KCNQ1-KD cells pre-treated with moxifloxacin 300 μM. (*D*, *E*) The effect of *KCNQ1* knock-down (KCNQ1-KD) and the I_{Kr} blocker moxifloxacin on APD_{90} (at 0.5 Hz). KCNQ1-KD cells exhibited significant prolongation of APD at baseline ($P < 0.0001$ vs. untreated control cells and $P = 0.31$ vs. untreated JLN cells) (*D*). Furthermore, pre-treatment with moxifloxacin (300 μM) resulted in further prolongation of APD in KCNQ1-KD cells ($P < 0.0001$ vs. pre-treated control cells and $P = 0.0007$ vs. pre-treated JLN cells) (*E*). (–) not significant, $^{**}P < 0.01$, $^{***}P < 0.001$, $^{****}P < 0.0001$ by Kruskal–Wallis test otherwise specified.

only a minor change in repolarization. In contrast, genetic ablation of *KCNQ1* through multiple approaches produced much greater increases in APD. This finding strongly supports the hypothesis that *KCNQ1* expression mediates cardiac repolarization by mechanisms beyond simply generating I_{Ks}.

In addition, exposure to the low-risk I_{Kr} blocker moxifloxacin produced little increase in APD_{90}, while the high-risk I_{Kr} blocker dofetilide generated significant APD prolongation in the iPSC-CMs. This differential effect may partially reflect a 'compensatory' increase in I_{Ks} by moxifloxacin, not seen with dofetilide. The qPCR data suggest a transcriptional increase in *KCNQ1* was responsible, and this is supported by the finding that the moxifloxacin-induced increase in I_{Ks} was not seen in iPSC-CMs in which *KCNQ1* expression was reduced or absent. iPSC-CMs demonstrate automaticity, heterogeneity, and immaturity compared to human ventricular myocytes. However, the amplitude of I_{Ks} in our population control cells was similar to that reported in healthy human left ventricular myocytes.[22] Taken together, these experiments also demonstrate that compensatory changes in multiple ionic currents that we documented in our previous work with *SCN5A* variants extend to response to drugs, and these occur relatively rapidly (over hours).

4.3 Potential mechanisms underlying *KCNQ1* effect

KCNQ1 expression clearly generates I_{Ks}, but our data also implicate mechanisms beyond this effect. One possibility is that while we and others show that I_{Ks} is small in human ventricular myocytes, it may be larger in other cell types, e.g. Purkinje. Interestingly, studies in genetically modified mice show that expression of the *KCNQ1* partner *KCNE1* is largely confined to the conduction system.[52–54]

A second possibility is that *KCNQ1* expression modulates the function of other key ion channels and data supporting an effect of $K_V7.1$ to act as a chaperone for I_{Kr} to support this idea.[27,55–57] In addition, Xiao *et al.* reported that dofetilide increased I_{Ks} without modifying I_{Kr} amplitude in adult canine left ventricular myocytes.[58] Ren *et al.* reported *KCNQ1* expression decreased I_{Kr} density in heterologous overexpression.[59] Thus, QT prolongation with at least some LOF variants of *KCNQ1* is generated not only by decreased I_{Ks} but also by decreased I_{Kr} availability. One approach we have evaluated to test this idea is to perform co-immunostaining for $K_V7.1$ and hERG in iPSC-CMs. However, we have found that $K_V7.1$ is expressed only at low abundance (<10% of hERG) in control cells. A third possibility is highlighted by recent experiments that implicate co-transcription or co-translation of major ion channels to co-ordinately modulate repolarization.[60] *KCNQ1* transcript may play a role in controlling *KCNH2* transcripts and/or trafficking of hERG in iPSC-CMs (*Figure 3F*). The I_{Kr} blocker moxifloxacin increases both *KCNQ1* and *KCNH2* transcripts through as-yet-undetermined mechanism(s). We observed up-regulated *KCNH2* and *KCNQ1* transcript with the two I_{Kr} blockers, comparably up-regulated $K_V7.1$ production, and a distinct effect on the increase in I_{Ks}. Therefore, we speculate that the differential effect of the two I_{Kr} blockers on the increase in I_{Ks} occurred between the protein production of $K_V7.1$

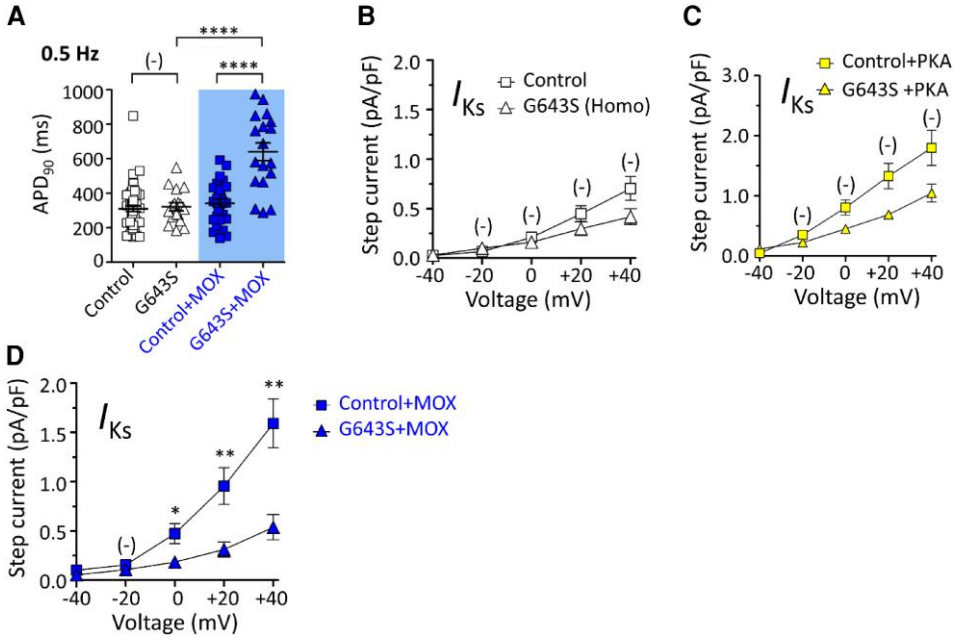

Figure 5 Effect of the common *KCNQ1* variant G643S on action potential duration and I_{Ks} with I_{Kr} blocker challenge. (*A*) APD_{90} in control and G643S cells at baseline (open squared and open triangles, respectively) and after chronic exposure to moxifloxacin (300 μM, blue squares and blue triangles, respectively) (at 0.5 Hz). ****$P < 0.0001$ by Kruskal–Wallis test. (*B*) The *I–V* relationship of baseline I_{Ks} in control ($n/N = 27/6$, open squares) and G643S cells ($n/N = 15/3$, open triangles). (*C*) The *I–V* relationship of I_{Ks} in response to acute PKA activation by IBMX and forskolin in control ($n/N = 10/3$, yellow squares) and G643S cells ($n/N = 8/2$, yellow triangles). (*D*) The *I–V* relationship of I_{Ks} in response to chronic treatment with moxifloxacin (300 μM) for 24–48 h in control ($n/N = 13/5$, blue squares) and G643S cells ($n/N = 11/3$, blue triangles). (–) not significant, *$P < 0.05$, **$P < 0.01$ by Mann–Whitney *U* test otherwise specified.

and transport/membrane expression of I_{Ks}. Our data on the G643S variant iPSC-CMs, which showed no increase in *KCNQ1* transcripts and I_{Ks} after moxifloxacin treatment, suggest that the molecular mechanism of the moxifloxacin-associated increase in the *KCNQ1* and the consequent electrophysiological remodeling may be initiated by the drug targeting a specific region of *KCNQ1* transcripts.

Translational perspective

Mutations in *KCNQ1*—whose expression generates I_{Ks}—are the major cause of long QT syndrome. We report here that while pharmacologic I_{Ks} block in human cardiomyocytes generates minimal change in repolarization, suppressing *KCNQ1* expression markedly increases both baseline repolarization duration and sensitivity to some (but not all) specific I_{Kr} blockers. Thus, beyond simply generating I_{Ks}, *KCNQ1* subserves critical additional role(s) in repolarization control at baseline and in response to I_{Kr} block. Our findings imply that the assessment of arrhythmic risk in individual patients and by drugs requires a framework that extends beyond a simple one gene-one ion current paradigm.

5. Limitations

As discussed above, the mechanisms underlying our findings remain to be completely defined. The extent to which the findings generalize to other I_{Kr} blockers is unknown. Assessing clinical diLQT risk for rare variants or even common variants like G643S is difficult because carriers also need to be exposed to at-risk drugs; even very large population datasets linking phenotypic information to genetic variants, like UK Biobank or *All of Us*, may not have the power to compare risk across the spectrum of *KCNQ1* rare variants in drug-exposed individuals.

6. Future directions

Conventional models focus on the idea that individual response to either genetic variants or blocking drugs affecting single ion channels can be readily translated to integrated effects at the level of APD or QT. Clinical observations, including variable QT responses to blocking drugs and variable penetrance in cLQTS families, support the idea that normal cardiac repolarization reflects the net effects of multiple ionic currents and that lesions affecting function of one (or more) of currents may remain subclinical until a 'final insult' of I_{Kr} block is superimposed. This is how the original concept of 'reduced repolarization reserve' was formulated. The data presented here highlight the idea that drug challenge itself, especially chronic exposure, may elicit compensatory changes that can protect against diLQT. Taken together, studies in iPSC-CMs are demonstrating that our view of cellular electrophysiology must evolve from one of a series of static ion currents to one that embraces dynamic interactions among currents and the pathways that control their expression and function.

7. Conclusions

Pharmacologic inhibition of I_{Ks} produces minimal changes in baseline APD_{90} in iPSC-CMs. In contrast, genetic ablation of *KCNQ1* produces

much greater APD_{90} increases. Chronic exposure to an I_{Kr} blocker with a low risk for TdP increases I_{Ks}, limiting the extent of APD_{90} prolongation; however, this effect is not seen after genetic ablation of *KCNQ1*, when I_{Kr} block markedly prolongs APD_{90}. These data strongly suggest that *KCNQ1* expression modulates baseline cardiac repolarization, and the response to I_{Kr} block, through mechanisms beyond simply generating I_{Ks}.

Supplementary material

Supplementary material is available at *Cardiovascular Research* online.

Acknowledgements

We thank Ashli E. Chew, B.S., for assistance with cell culture, and Teresa L. Strickland, R.N., B.S.N., for patients' sample collection. Flow Cytometry experiments were performed in the Vanderbilt Flow Cytometry Shared Resource supported by the Vanderbilt Ingram Cancer Center (P30 CA068485) and the Vanderbilt Digestive Disease Research Center (DK058404).

Conflict of interest: All authors report no conflict of interest.

Funding

This project was supported by National Institutes of Health (R01 HL149826 and HL164675 to D.M.R., R00 HG010904 and R35 GM150465 to A.M.G.), the Heart Rhythm Society (Clinical Research Award in Honor of Mark Josephson and Hein Wellens to Y.W.), and the American Heart Association (postdoctoral fellowship #830951 and career development award # 23CDA1048873 to Y.W.).

Data availability

The data that support the findings of this study are available from the corresponding author upon reasonable request.

References

1. Franco D, Demolombe S, Kupershmidt S, Dumaine R, Dominguez JN, Roden D, Antzelevitch C, Escande D, Moorman AFM. Divergent expression of delayed rectifier K+ channel subunits during mouse heart development. *Cardiovasc Res* 2001;**52**:65–75. PMID: 11557234.
2. Nerbonne JM, Kass RS. Molecular physiology of cardiac repolarization. *Physiol Rev* 2005;**85**: 1205–1253. PMID:16183911.
3. Schwartz PJ, Crotti L, Insolia R. Long-QT syndrome: from genetics to management. *Circ Arrhythm Electrophysiol* 2012;**5**:868–877. PMID:22895603. PMC3461497.
4. Adler A, Novelli V, Amin AS, Abiusi E, Care M, Nannenberg EA, Feilotter H, Amenta S, Mazza D, Bikker H, Sturm AC, Garcia J, Ackerman MJ, Hershberger RE, Perez MV, Zareba W, Ware JS, Wilde AAM, Gollob MH. An international, multicentered, evidence-based reappraisal of genes reported to cause congenital long QT syndrome. *Circulation* 2020;**141**:418–428. PMID:31983240. PMC7017940.
5. Jervell A, Lange-Nielsen F. Congenital deaf-mutism, functional heart disease with prolongation of the Q-T interval and sudden death. *Am Heart J* 1957;**54**:59–68. PMID:13435203.
6. Schwartz PJ, Spazzolini C, Crotti L, Bathen J, Amlie JP, Timothy K, Shkolnikova M, Berul CI, Bitner-Glindzicz M, Toivonen L, Horie M, Schulze-Bahr E, Denjoy I. The Jervell and Lange-Nielsen syndrome: natural history, molecular basis, and clinical outcome. *Circulation* 2006;**113**:783–790.
7. Roden DM. Drug-induced prolongation of the QT interval. *N Engl J Med* 2004;**350**: 1013–1022. PMID:14999113.
8. Lu HR, Vlaminckx E, Van Ammel K, De Clerck F. Drug-induced long QT in isolated rabbit Purkinje fibers: importance of action potential duration, triangulation and early afterdepolarizations. *Eur J Pharmacol* 2002;**452**:183–192. PMID:12354568.
9. Sims C, Reisenweber S, Viswanathan PC, Choi B-R, Walker WH, Salama G. Sex, age, and regional differences in L-type calcium current are important determinants of arrhythmia phenotype in rabbit hearts with drug-induced long QT type 2. *Circ Res* 2008;**102**: e86–e100. PMID:18436794. PMC2737508.
10. Lahti AL, Kujala VJ, Chapman H, Koivisto A-P, Pekkanen-Mattila M, Kerkelä E, Hyttinen J, Kontula K, Swan H, Conklin BR, Yamanaka S, Silvennoinen O, Aalto-Setälä K. Model for long QT syndrome type 2 using human iPS cells demonstrates arrhythmogenic characteristics in cell culture. *Dis Model Mech* 2012;**5**:220–230. PMID:22052944. PMC3291643.
11. Bellin M, Casini S, Davis RP, D'Aniello C, Haas J, Ward-van Oostwaard D, Tertoolen LGJ, Jung CB, Elliott DA, Welling A, Laugwitz K-L, Moretti A, Mummery CL. Isogenic human pluripotent stem cell pairs reveal the role of a KCNH2 mutation in long-QT syndrome. *EMBO J* 2013;**32**:3161–3175.
12. Blinova K, Stohlman J, Vicente J, Chan D, Johannesen L, Hortigon-Vinagre MP, Zamora V, Smith G, Crumb WJ, Pang L, Lyn-Cook B, Ross J, Brock M, Chvatal S, Millard D, Galeotti L, Stockbridge N, Strauss DG. Comprehensive translational assessment of human-induced pluripotent stem cell derived cardiomyocytes for evaluating drug-induced arrhythmias. *Toxicol Sci* 2017;**155**:234–247. PMID:27701120. PMC6093617.
13. Stillitano F, Hansen J, Kong C-W, Karakikes I, Funck-Brentano C, Geng L, Scott S, Reynier S, Wu M, Valogne Y, Desseaux C, Salem J-E, Jeziorowska D, Zahr N, Li R, Iyengar R, Hajjar RJ, Hulot J-S. Modeling susceptibility to drug-induced long QT with a panel of subject-specific induced pluripotent stem cells. *Elife* 2017;**6**:e19406, PMID:28134617. PMC5279943.
14. Wang Z, Tristani-Firouzi M, Xu Q, Lin M, Keating MT, Sanguinetti MC. Functional effects of mutations in KvLQT1 that cause long QT syndrome. *J Cardiovasc Electrophysiol* 1999;**10**: 817–826. PMID:10376919.
15. Moss AJ, Shimizu W, Wilde AAM, Towbin JA, Zareba W, Robinson JL, Qi M, Vincent GM, Ackerman MJ, Kaufman ES, Hofman N, Seth R, Kamakura S, Miyamoto Y, Goldenberg I, Andrews ML, McNitt S. Clinical aspects of type-1 long-QT syndrome by location, coding type, and biophysical function of mutations involving the KCNQ1 gene. *Circulation* 2007; **115**:2481–2489. PMID:17470695. PMC3332528.
16. Casimiro MC, Knollmann BC, Ebert SN, Vary JC Jr, Greene AE, Franz MR, Grinberg A, Huang SP, Pfeifer K. Targeted disruption of the Kcnq1 gene produces a mouse model of Jervell and Lange-Nielsen syndrome. *Proc Natl Acad Sci U S A* 2001;**98**:2526–2531. PMID:11226272. PMC30171.
17. Brunner M, Peng X, Liu GX, Ren X-Q, Ziv O, Choi B-R, Mathur R, Hajjiri M, Odening KE, Steinberg E, Folco EJ, Pringa E, Centracchio J, Macharzina RR, Donahay T, Schofield L, Rana N, Kirk M, Mitchell GF, Poppas A, Zehender M, Koren G. Mechanisms of cardiac arrhythmias and sudden death in transgenic rabbits with long QT syndrome. *J Clin Invest* 2008;**118**:2246–2259. PMID:18464931. PMC2373420.
18. Aiba T, Shimizu W, Inagaki M, Noda T, Miyoshi S, Ding W-G, Zankov DP, Toyoda F, Matsuura H, Horie M, Sunagawa K. Cellular and ionic mechanism for drug-induced long QT syndrome and effectiveness of verapamil. *J Am Coll Cardiol* 2005;**45**:300–307. PMID: 15653031.
19. Zhang M, D'Aniello C, Verkerk AO, Wrobel E, Frank S, Ward-van Oostwaard D, Piccini I, Freund C, Rao J, Seebohm G, Atsma DE, Schulze-Bahr E, Mummery CL, Greber B, Bellin M. Recessive cardiac phenotypes in induced pluripotent stem cell models of Jervell and Lange-Nielsen syndrome: disease mechanisms and pharmacological rescue. *Proc Natl Acad Sci U S A* 2014;**111**:E5383–E5392. PMID:25453094. PMC4273331.
20. O'Hara T, Rudy Y. Arrhythmia formation in subclinical ("silent") long QT syndrome requires multiple insults: quantitative mechanistic study using the KCNQ1 mutation Q357R as example. *Heart Rhythm* 2012;**9**:275–282. PMID:21952006. PMC3443981.
21. Varró A, Baláti B, Iost N, Takács J, Virág L, Lathrop DA, Csaba L, Tálosi L, Papp JG. The role of the delayed rectifier component I_{Ks} in dog ventricular muscle and Purkinje fibre repolarization. *J Physiol* 2000;**523**:67–81.
22. Jost N, Virág L, Bitay M, Takács J, Lengyel C, Biliczki P, Nagy Z, Bogáts G, Lathrop DA, Papp JG, Varró A. Restricting excessive cardiac action potential and QT prolongation: a vital role for IKs in human ventricular muscle. *Circulation* 2005;**112**:1392–1399. PMID:16129791.
23. Zhang X, Guo L, Zeng H, White SL, Furniss M, Balasubramanian B, Lis E, Lagrutta A, Sannajust F, Zhao LL, Xi B, Wang X, Davis M, Abassi YA. Multi-parametric assessment of cardiomyocyte excitation-contraction coupling using impedance and field potential recording: a tool for cardiac safety assessment. *J Pharmacol Toxicol Methods* 2016;**81**:201–216.
24. Lengyel C, Varró A, Tábori K, Papp JG, Baczkó I. Combined pharmacological block of I_{Kr} and I_{Ks} increases short-term QT interval variability and provokes torsades de pointes. *Br J Pharmacol* 2007;**151**:941–951.
25. Zeng H, Wang J, Clouse H, Lagrutta A, Sannajust F. Human-induced pluripotent stem cell-derived cardiomyocytes have limited IKs for repolarization reserve as revealed by specific KCNQ1/KCNE1 blocker. *JRSM Cardiovasc Dis* 2019;**8**:2048004019854919. PMID: 31217965. PMC6558757.
26. Yamashita F, Horie M, Kubota T, Yoshida H, Yumoto Y, Kobori A, Ninomiya T, Kono Y, Haruna T, Tsuji K, Washizuka T, Takano M, Otani H, Sasayama S, Aizawa Y. Characterization and subcellular localization of KCNQ1 with a heterozygous mutation in the C terminus. *J Mol Cell Cardiol* 2001;**33**:197–207. PMID:11162126.
27. Biliczki P, Girmatsion Z, Brandes RP, Harenkamp S, Pitard B, Charpentier F, Hébert TE, Hohnloser SH, Baró I, Nattel S, Ehrlich JR. Trafficking-deficient long QT syndrome mutation KCNQ1-T587M confers severe clinical phenotype by impairment of KCNH2 membrane localization: evidence for clinically significant IKr-IKs α-subunit interaction. *Heart Rhythm* 2009; **6**:1792–1801.
28. Lee Y-K, Sala L, Mura M, Rocchetti M, Pedrazzini M, Ran X, Mak TSH, Crotti L, Sham PC, Torre E, Zaza A, Schwartz PJ, Tse H-F, Gnecchi M. *MTMR4* SNVs modulate ion channel degradation and clinical severity in congenital long QT syndrome: insights in the mechanism of action of protective modifier genes. *Cardiovasc Res* 2021;**117**:767–779.
29. Wada Y, Yang T, Shaffer CM, Daniel LL, Glazer AM, Davogustto GE, Lowery BD, Farber-Eger EH, Wells QS, Roden DM. Common ancestry-specific ion channel variants predispose to drug-induced arrhythmias. *Circulation* 2022;**145**:299–308. PMID:34994586. PMC8852297.
30. So PP-S, Backx PH, Dorian P. Slow delayed rectifier K+ current block by HMR 1556 increases dispersion of repolarization and promotes Torsades de Pointes in rabbit ventricles. *Br J Pharmacol* 2008;**155**:1185–1194. PMID:18836478. PMC2607203.
31. Thomas GP, Gerlach U, Antzelevitch C. HMR 1556, a potent and selective blocker of slowly activating delayed rectifier potassium current. *J Cardiovasc Pharmacol* 2003;**41**:140–147. PMID:12500032.

32. Nicolas CS, Park K-H, El Harchi A, Camonis J, Kass RS, Escande D, Mérot J, Loussouarn G, Le Bouffant F, Baró I. IKs response to protein kinase A-dependent KCNQ1 phosphorylation requires direct interaction with microtubules. *Cardiovasc Res* 2008;**79**:427–435. PMID: 18390900. PMC2781743.
33. Thompson E, Eldstrom J, Westhoff M, McAfee D, Balse E, Fedida D. cAMP-dependent regulation of IKs single-channel kinetics. *J Gen Physiol* 2017;**149**:781–798. PMID:28687606. PMC5560775.
34. Bersell K, Montgomery JA, Kanagasundram AN, Campbell CM, Chung WK, Macaya D, Konecki D, Venter E, Shoemaker MB, Roden DM. Partial duplication and poly(A) insertion in KCNQ1 not detected by next-generation sequencing in Jervell and Lange-Nielsen syndrome. *Circ Arrhythm Electrophysiol* 2016;**9**:e004081.
35. Yang T, Chun YW, Stroud DM, Mosley JD, Knollmann BC, Hong C, Roden DM. Screening for acute IKr block is insufficient to detect torsades de pointes liability: role of late sodium current. *Circulation* 2014;**130**:224–234. PMID:24895457. PMC4101031.
36. Lu Z, Wu C-YC, Jiang Y-P, Ballou LM, Clausen C, Cohen IS, Lin RZ. Suppression of phosphoinositide 3-kinase signaling and alteration of multiple ion currents in drug-induced long QT syndrome. *Sci Transl Med* 2012;**4**:131ra50. PMID:22539774. PMC3494282.
37. Démolis JL, Kubitza D, Tennezé L, Funck-Brentano C. Effect of a single oral dose of moxifloxacin (400 mg and 800 mg) on ventricular repolarization in healthy subjects. *Clin Pharmacol Ther* 2000;**68**:658–666. PMID:11180026.
38. Qiu XS, Chauveau S, Anyukhovsky EP, Rahim T, Jiang Y-P, Harleton E, Feinmark SJ, Lin RZ, Coronel R, Janse MJ, Opthof T, Rosen TS, Cohen IS, Rosen MR. Increased late sodium current contributes to the electrophysiological effects of chronic, but not acute, dofetilide administration. *Circ Arrhythm Electrophysiol* 2016;**9**:e003655. PMID:27071826. PMC4850912.
39. Kubota T, Horie M, Takano M, Yoshida H, Takenaka K, Watanabe E, Tsuchiya T, Otani H, Sasayama S. Evidence for a single nucleotide polymorphism in the KCNQ1 potassium channel that underlies susceptibility to life-threatening arrhythmias. *J Cardiovasc Electrophysiol* 2001;**12**:1223–1229. PMID:11761407.
40. Nagasawa S, Saitoh H, Kasahara S, Chiba F, Torimitsu S, Abe H, Yajima D, Iwase H. Relationship between KCNQ1 (LQT1) and KCNH2 (LQT2) gene mutations and sudden death during illegal drug use. *Sci Rep* 2018;**8**:8443.
41. Curran ME, Splawski I, Timothy KW, Vincent GM, Green ED, Keating MT. A molecular basis for cardiac arrhythmia: HERG mutations cause long QT syndrome. *Cell* 1995;**80**:795–803. PMID:7889573.
42. Sanguinetti MC, Jiang C, Curran ME, Keating MT. A mechanistic link between an inherited and an acquired cardiac arrhythmia: HERG encodes the IKr potassium channel. *Cell* 1995; **81**:299–307. PMID:7736582.
43. Wang Q, Shen J, Splawski I, Atkinson D, Li Z, Robinson JL, Moss AJ, Towbin JA, Keating MT. SCN5A mutations associated with an inherited cardiac arrhythmia, long QT syndrome. *Cell* 1995;**80**:805–811. PMID:7889574.
44. Wang Q, Curran ME, Splawski I, Burn TC, Millholland JM, VanRaay TJ, Shen J, Timothy KW, Vincent GM, de Jager T, Schwartz PJ, Toubin JA, Moss AJ, Atkinson DL, Landes GM, Connors TD, Keating MT. Positional cloning of a novel potassium channel gene: KVLQT1 mutations cause cardiac arrhythmias. *Nat Genet* 1996;**12**:17–23.
45. Mitcheson JS, Chen J, Lin M, Culberson C, Sanguinetti MC. A structural basis for drug-induced long QT syndrome. *Proc Natl Acad Sci U S A* 2000;**97**:12329–12333. PMID: 11005845. PMC17341.
46. Splawski I, Timothy KW, Sharpe LM, Decher N, Kumar P, Bloise R, Napolitano C, Schwartz PJ, Joseph RM, Condouris K, Tager-Flusberg H, Priori SG, Sanguinetti MC, Keating MT. Ca(V) 1.2 calcium channel dysfunction causes a multisystem disorder including arrhythmia and autism. *Cell* 2004;**119**:19–31. PMID:15454078.
47. Ramirez AH, Shaffer CM, Delaney JT, Sexton DP, Levy SE, Rieder MJ, Nickerson DA, George AL Jr, Roden DM. Novel rare variants in congenital cardiac arrhythmia genes are frequent in drug-induced torsades de pointes. *Pharmacogenomics J* 2013;**13**:325–329. PMID:22584458. PMC3422407.
48. Weeke P, Mosley JD, Hanna D, Delaney JT, Shaffer C, Wells QS, Van Driest S, Karnes JH, Ingram C, Guo Y, Shyr Y, Norris K, Kannankeril PJ, Ramirez AH, Smith JD, Mardis ER, Nickerson D, George AL Jr, Roden DM. Exome sequencing implicates an increased burden of rare potassium channel variants in the risk of drug-induced long QT interval syndrome. *J Am Coll Cardiol* 2014;**63**:1430–1437. PMID:24561134. PMC4018823.
49. Itoh H, Crotti L, Aiba T, Spazzolini C, Denjoy I, Fressart V, Hayashi K, Nakajima T, Ohno S, Makiyama T, Wu J, Hasegawa K, Mastantuono E, Dagradi F, Pedrazzini M, Yamagishi M, Berthet M, Murakami Y, Shimizu W, Guicheney P, Schwartz PJ, Horie M. The genetics underlying acquired long QT syndrome: impact for genetic screening. *Eur Heart J* 2016;**37**: 1456–1464. PMID:26715165. PMC4914885.
50. Glazer AM, Davogustto G, Shaffer CM, Vanoye CG, Desai RR, Farber-Eger EH, Dikilitas O, Shang N, Pacheco JA, Yang T, Muhammad A, Mosley JD, Van Driest SL, Wells QS, Shaffer LL, Kalash OR, Wada Y, Bland HT, Yoneda ZT, Mitchell DW, Kroncke BM, Kullo IJ, Jarvik GP, Gordon AS, Larson EB, Manolio TA, Mirshahi T, Luo JZ, Schaid D, Namjou B, Alsaied T, Singh R, Singhal A, Liu C, Weng C, Hripcsak G, Ralston JD, McNally EM, Chung WK, Carrell DS, Leppig KA, Hakonarson H, Sleiman P, Sohn S, Glessner J, eMERGE Network, Denny J, Wei W-Q, George AL Jr, Shoemaker MB, Roden DM. Arrhythmia variant associations and reclassifications in the eMERGE-III sequencing study. *Circulation* 2022;**145**:877–891. PMID: 34930020. PMC8940719.
51. Strauss DG, Vicente J, Johannesen L, Blinova K, Mason JW, Weeke P, Behr ER, Roden DM, Woosley R, Kosova G, Rosenberg MA, Newton-Cheh C. Common genetic variant risk score is associated with drug-induced qt prolongation and torsade de pointes risk: a pilot study. *Circulation* 2017;**135**:1300–1310. PMID:28213480. PMC5380476.
52. Temple J, Frias P, Rottman J, Yang T, Wu Y, Verheijck EE, Zhang W, Siprachanh C, Kanki H, Atkinson JB, King P, Anderson ME, Kupershmidt S, Roden DM. Atrial fibrillation in KCNE1-null mice. *Circ Res* 2005;**97**:62–69
53. Moskowitz IPG, Pizard A, Patel VV, Bruneau BG, Kim JB, Kupershmidt S, Roden D, Berul CI, Seidman CE, Seidman JG. The T-Box transcription factor Tbx5 is required for the patterning and maturation of the murine cardiac conduction system. *Development* 2004;**131**: 4107–4116. PMID:15289437.
54. Kim EE, Shekhar A, Lu J, Lin X, Liu F-Y, Zhang J, Delmar M, Fishman GI. PCP4 regulates Purkinje cell excitability and cardiac rhythmicity. *J Clin Invest* 2014;**124**:5027–5036. PMID: 25295538. PMC4321194.
55. Guo J, Wang T, Yang T, Xu J, Li W, Fridman MD, Fisher JT, Zhang S. Interaction between the cardiac rapidly (IKr) and slowly (IKs) activating delayed rectifier potassium channels revealed by low K+-induced hERG endocytic degradation. *J Biol Chem* 2011;**286**:34664–34674. PMID:21844197. PMC3186392.
56. Organ-Darling LE, Vernon AN, Giovanniello JR, Lu Y, Moshal K, Roder K, Li W, Koren G. Interactions between hERG and KCNQ1 α-subunits are mediated by their COOH termini and modulated by cAMP. *Am J Physiol Heart Circ Physiol* 2013;**304**:H589–H599.
57. Wu J, Sakaguchi T, Takenaka K, Toyoda F, Tsuji K, Matsuura H, Horie M. A trafficking-deficient KCNQ1 mutation, T587M, causes a severe phenotype of long QT syndrome by interfering with intracellular hERG transport. *J Cardiol* 2019;**73**:343–350. PMID:30591322.
58. Xiao L, Xiao J, Luo X, Lin H, Wang Z, Nattel S. Feedback remodeling of cardiac potassium current expression. *Circulation* 2008;**118**:983–992.
59. Ren X-Q, Liu GX, Organ-Darling LE, Zheng R, Roder K, Jindal HK, Centracchio J, McDonald TV, Koren G. Pore mutants of HERG and KvLQT1 downregulate the reciprocal currents in stable cell lines. *Am J Physiol Heart Circ Physiol* 2010;**299**:H1525–H1534. PMID:20833965. PMC2993209.
60. Eichel CA, Ríos-Pérez EB, Liu F, Jameson MB, Jones DK, Knickelbine JJ, Robertson GA. A microtranslatome coordinately regulates sodium and potassium currents in the human heart. *Elife* 2019;**8**:e52654.